International Journal of Impact Engineering 111 (2018) 85–93

Contents lists available at ScienceDirect

International Journal of Impact Engineering

journal homepage: www.elsevier.com/locate/ijimpeng

Low-velocity impact performance and effect factor analysis of scarf-repaired composite laminates

Xiaoquan Cheng[a,*], Jie Zhang[a], Jianwen Bao[b], Benyin Zeng[c], Yujia Cheng[a], Renwei Hu[a]

[a] School of Aeronautic Science and Engineering, Beihang University, Beijing, 100191, China
[b] Science and Technology on Advanced Composites Laboratory, BIAM, AVIC Composite Center, AVIC Composite Corporation LTD, Beijing, 100095, China
[c] Helicopter Research and Development Institute, Aviation Industry Corporation of China, Jingdezhen, 333001, China

ARTICLE INFO

Article History:
Received 10 January 2017
Revised 16 August 2017
Accepted 6 September 2017
Available online 8 September 2017

Keywords:
Composite scarf-repaired laminate
Continuum damage mechanics
Impact behavior
Damage mechanism
Configurational parameters

ABSTRACT

Low-velocity impact performance of scarf-repaired composite laminates was investigated by experimental and numerical methods. The numerical model was built using continuum damage mechanics and cohesive elements were used in all the interfaces of the adherends (i.e. the patch and the parent). The model was verified to be efficient. Based on it, damage profiles and damage mechanism were studied, and the effects of the scarf angle, the adhesive thickness and the patch off-axis angles were analyzed. Results show that the patch damage occurs in its center region through the thickness, while the damages in the parent and adhesive mainly occur around the back face. Damage area of the patch is obviously more serious than that of the parent, and the adhesive can protect the parent to some degree. The scarf angle, the adhesive thickness and the patch off-axis angles have effects on the impact properties. The scarf angles ranging from 7° to 8°, the adhesive thicknesses of 0.15 mm, the patch off-axis angles ranging from 135° to 160° are recommended for better impact performances.

1. Introduction

Low-velocity impact could cause various damages in composite laminated structure, such as fiber breakage, matrix cracking, shear failure and delamination [1]. Such damages, especially delamination, can cause significant reduction in structural integrity and residual compressive strength [2]. Compared with intact laminate, impact behavior of scarf-repaired laminate is more complicated due to the introduction of scarf joint [3].

There have been sufficient literatures about impact behavior investigations of composite scarf joints, in which most researches are about 2D scarf joints [4–8]. Compared with 3D scarf-repaired structure, 2D scarf joint structures are simpler, and their loading transfer across the adhesive and the bonding interfaces is not so complicated. The numerical modeling of 2D scarf joint is much easier, and 2D scarf joint hardly reflects damage mechanism of 3D scarf repaired structure. Some studies have been carried out on impact behavior of scarf-repaired structures. Chotard et al. [9] experimentally explored impact properties of scarf-repaired box-shape composite structure and compared mechanical properties of intact, impact-damaged and repaired structures. They found that scarf repair is an efficient repair method which can achieve more impact stiffness and strength than intact structure, and fatigue life of repaired structure can reach 3.5 times of that of impact-damaged structure. Takahashi et al. [10] used lamb wave sensing to detect impact damages in scarf-repaired laminates and concluded that the debonding between the adhesive and adherends (parent and patch) arises from the shear failures and delamination in the patch near the impact point. Cheng et al. [11,12] investigated impact behavior and post-impact properties of scarf-repaired composite laminates with different impact energies and locations by experiment. Results show that larger impact energy causes larger ultimate impact force and damage area. The damage area is largest and residual compressive strength is smallest when impact location is at the bondline.

Impact behavior of scarf-repaired structures is primarily investigated by experiment and the effects of repair configurational parameters on it are hardly studied. Relevant numerical stimulation is extremely required for saving experimental cost and exploring failure mechanism. However, most current numerical investigations of composite impact behavior are limited to intact laminates with little attention to scarf-repaired laminates. And, impact simulation of intact laminates has been relatively mature, in which continuum damage mechanics is widely used [13–16]. The principle of this approach is that damage variables are introduced corresponding to damage modes, and continuous damage degradation was achieved by continuous variation of damage variables. Compared with intact laminates, adhesive and scarf interfaces are introduced in scarf-repaired laminates, which inevitably increases the difficulty of modeling.

* Corresponding author.
E-mail address: xiaoquan_cheng@buaa.edu.cn (X. Cheng).

http://dx.doi.org/10.1016/j.ijimpeng.2017.09.004
0734-743X/

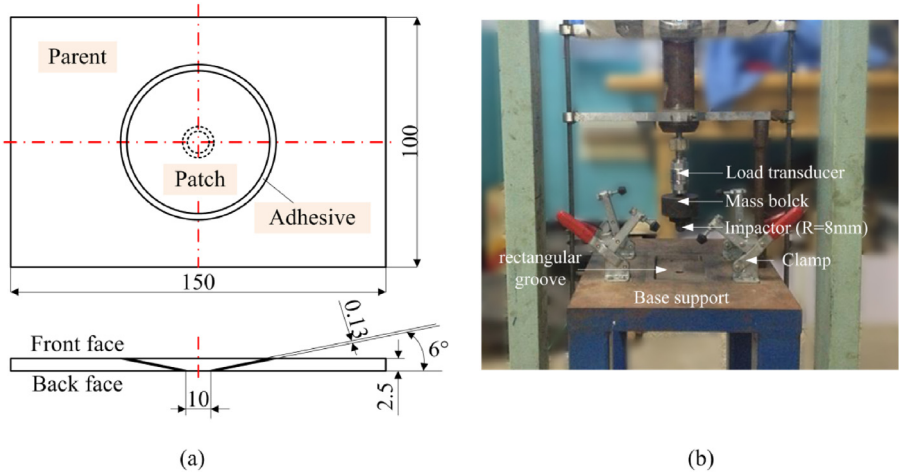

Fig. 1. Experimental conditions. (a) Specimen geometry (unit: mm); (b) drop weight impact test fixture.

In this paper, impact experiment of scarf-repaired laminate was performed and relevant 3D numerical model was established using continuum damage mechanics. Based on the model, damage mechanism was studied, and the effects of scarf angle, adhesive thickness and patch off-axis angles were analyzed.

2. Experimental procedure

Scarf-repaired composite laminate consists of adherends (i.e. parent and patch) and adhesive. Both of the adherends here were made of CCF300/5228A (carbon fiber/epoxy) with stacking sequence of $[45/0_2/-45/90/45/0_2/-45/0]_s$. A layer of adhesive film with nominal thickness of 0.13 mm was used and its material is SY-14. Detailed specimen geometry is shown in Fig. 1(a).

Drop weight impact test was performed based on ASTM D7137 [17] and its fixture is shown in Fig. 1(b). The impactor is a steel hemisphere with radius of 8 mm, and the total mass of drop objects is 5.5 kg. The impact point was at the patch center, and the impact energies were 4.45 J/mm and 6.67 J/mm. The specimen was clamped on the base support at four points. Impact force between the impactor and the specimen was recorded by load transducer during the whole impact process, and the damage was detected by ultrasonic C-scan device.

3. Numerical model

3.1. Damage simulation

The impact system includes adherends, adhesive and impactor, etc. Impactor damage was neglected as there is no damage to the impactor in the experiment. The damage simulations of adherends and adhesive would be illustrated in this section.

3.1.1. Adherends

Four damage modes were considered for the adherends: fiber breakage (tension/compression), matrix cracking (tension/compression), fiber-matrix shear failure (two in-plane and one out-of-plane failures) and delamination (mixed mode I, II and III). Based on the continuum damage mechanics, the first three damage modes were modeled by subroutine VUMAT in ABAQUS, and the calculation process of VUMAT is shown in Fig. 2. The damage criteria of fiber breakage and matrix cracking were strain-based Hashin criteria [18], as shown in Eqs. (1)–(4). Nonlinear shear damage model based on the in-plane shear test [14] was used to describe the fiber-matrix shear failures as shown in Fig. 3(b). Damage criterion of the shear failures was maximum shear strain criterion, as shown in Eq. (5), and the maximum shear strain γ_{pq}^0 ($pq = 12, 23, 31$) was 5% according to ASTM D3518 [19]. The constitutive relations of the shear failures were simulated by exponential functions (see Fig. 3(b)) when $\gamma < \gamma_{pq}^0$ [20].

$$(f_{ft})^2 = \left(\frac{\varepsilon_{11}}{X_T}E_{11}\right)^2 + \left(\frac{\gamma_{12}}{S_{12}}G_{12}\right)^2 + \left(\frac{\gamma_{31}}{S_{31}}G_{31}\right)^2 \geq 1 \quad \text{if} \quad \varepsilon_{11} > 0 \tag{1}$$

$$(f_{fc})^2 = \left(\frac{\varepsilon_{11}}{X_C}E_{11}\right)^2 \geq 1 \quad \text{if} \quad \varepsilon_{11} \leq 0 \tag{2}$$

$$(f_{mt})^2 = \left(\frac{\varepsilon_{22}+\varepsilon_{33}}{Y_T}E_{22}\right)^2 - \frac{\varepsilon_{22}\varepsilon_{33}}{S_{23}^2}E_{22}^2 + \left(\frac{\gamma_{12}}{S_{12}}G_{12}\right)^2 + \left(\frac{\gamma_{23}}{S_{23}}G_{23}\right)^2 + \left(\frac{\gamma_{31}}{S_{31}}G_{31}\right)^2 \geq 1 \quad \text{if } \varepsilon_{22}+\varepsilon_{33} > 0 \tag{3}$$

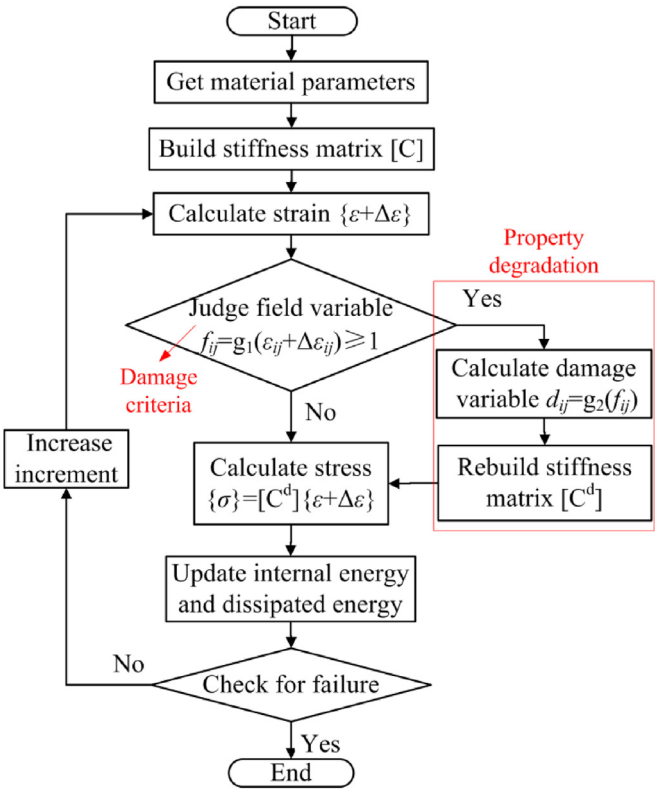

Fig. 2. Calculation process of subroutine VUMAT.